

# Applications of the SCENIC code package to the minority ion-cyclotron heating in Wendelstein 7-X plasmas

J.M. Faustin\*, W.A. Cooper\*, J. Geiger<sup>†</sup>, J.P. Graves\* and D. Pfefferlé\*

\*Ecole Polytechnique Fédérale de Lausanne (EPFL), Centre de Recherches en Physique des Plasmas (CRPP),  
CH-1015 Lausanne, Switzerland

<sup>†</sup>Max-Planck Institut für Plasmaphysik, D-17491 Greifswald, Germany

**Abstract.** We present SCENIC simulations of a W7X 4He plasma with 1% H minority and with an antenna model close to the design foreseen for the W7X ICRF antenna [1, 2]. A high mirror and a standard equilibrium are considered. The injected wave frequency is fixed at 33.8 MHz and 39.6MHz respectively and only fundamental minority heating is considered. Included in this calculation is a new realistic model of the antenna, where it is found that the localization of the antenna geometry tends to break the five-fold periodicity of the system. We assess the heat transfer through the toroidal periods via Coulomb collisions.

**Keywords:** Stellarator, ICRH, Monte Carlo simulations

**PACS:** 52.55.Hc, 52.50.Qt, 52.65Pp, 52.65Cc

## INTRODUCTION

Wendelstein 7-X (W7X) is a large superconducting approximately quasi-isodynamic stellarator design under construction in Greifswald, Germany. Several sources of heating will be mixed in W7X in order to reach fusion plasma relevant temperatures. An assessment of the viability of ion-cyclotron resonance heating (ICRH) applied to W7X constitutes an important step to determine whether this approach is feasible. The design of antennas for this method of heating relies heavily on ICRH simulations of quasi-isodynamic stellarator systems. The main features of the ICRH system for W7X are already known [1, 2]. During the first operation phase involving ICRH only one antenna located near a bean-shaped cross section will be used. We apply the SCENIC package<sup>1</sup> to fundamental ICRH minority heating scenario of <sup>4</sup>He(H) plasmas with  $n_H/n_e = 1\%$ . Electron central density is chosen as  $n_{e0} = 8 \times 10^{19} m^{-3}$  and the electron and ion profiles take the form  $n_{e,i}(s) = n_{e,i0} (0.9(1 - s^4)^4 + 0.1)$ . We compute the wave field with a new realistic model of the antenna using the 3D full wave code LEMan [5, 6]. The wave numbers and electric field are passed to the orbit following code VENUS-LEVIS [7] to solve for the minority distribution functions. We compare the power deposition to the plasma background in two types of equilibria characterised by diverse mirror ratios.

## EQUILIBRIA

The equilibrium code ANIMEC is used to compute the fixed boundary isotropic 3D W7X equilibria. The currents flowing in the modular and planar coils of W7X fully define the MHD equilibrium and allow flexible access to various types of toroidal mirror ratio [8] :

$$\frac{B_{\varphi=0} - B_{\varphi=\pi/5}}{B_{\varphi=0} + B_{\varphi=\pi/5}} \quad (1)$$

In equation 1,  $\varphi$  labels the toroidal angle and  $\varphi = 0$  is taken at the bean-shaped cross section. We investigate two particular equilibria whose rotational transform  $t$  are given in Figure 1, where  $s$  is the toroidal magnetic flux normalised

---

<sup>1</sup> The SCENIC code package [3] comprises three components. The ANIMEC code (Anisotropic Neumann Inverse Method Equilibrium Code) [4] is used to compute a W7X fixed boundary 3D geometry with full-shaping plasma equilibrium. The 3D full wave code LEMan (Low frequency ElectroMagnetic wave propagation) [5, 6] reads this equilibrium and computes the wave field in the ion-cyclotron range of frequency with warm contributions to the dielectric tensor. The wave numbers and electric field are passed to the VENUS-LEVIS code [7] that evolves the minority species particles guiding centre orbits.

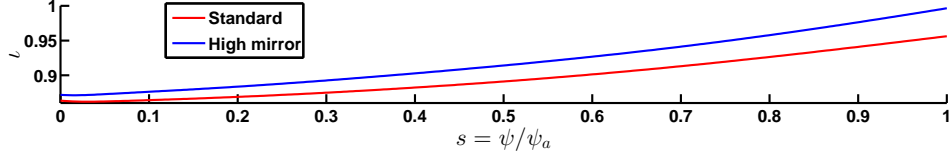


FIGURE 1. Rotational transform profiles for the standard and the high mirror equilibria configuration.

to its edge value  $\psi_a$  and is thus proportional to the enclosed plasma volume. The mirror ratios of the so-called high- and standard-mirror cases are respectively 8.7% and 4%. The high mirror configuration displays a peculiar feature concerning the wave propagation. The minimum magnetic field in the bean-shaped cross section is higher than the maximum magnetic field in the triangular cross section. Therefore no wave frequency matching a resonant field can be found at every toroidal angle.

## FULL-WAVE CALCULATION

The equilibrium computed by ANIMEC for each magnetic configuration, is converted into Boozer coordinates and read by the LEMan code for the full-wave calculation. The geometry of the antenna is known from Ref. [2] and modelled by a new module in the LEMan code which approximates a local antenna. The antenna frequency has to be chosen carefully for each equilibria because of the large discrepancy in their magnetic field profile.

**High mirror configuration :** a preliminary study of the wave deposition using a global antenna, i.e. containing only one mode  $(m, n)$  has already been done for the high mirror configuration [9]. These preliminary results indicated that an antenna frequency around 33.8 MHz corresponding to a resonant field of 2.22T gives an optimal power deposition in the plasma centre compared to the edge. In the following the localised antenna frequency will therefore be set to this frequency for the high mirror configuration.

**Standard configuration :** the frequency is chosen in order to take advantage of the lower mirror ratio. The antenna frequency is therefore set to 39.6 MHz which gives a fairly good power deposition in the plasma centre as shown in the next section. This frequency corresponds to a resonant magnetic field value of 2.6T and is present at every toroidal angle.

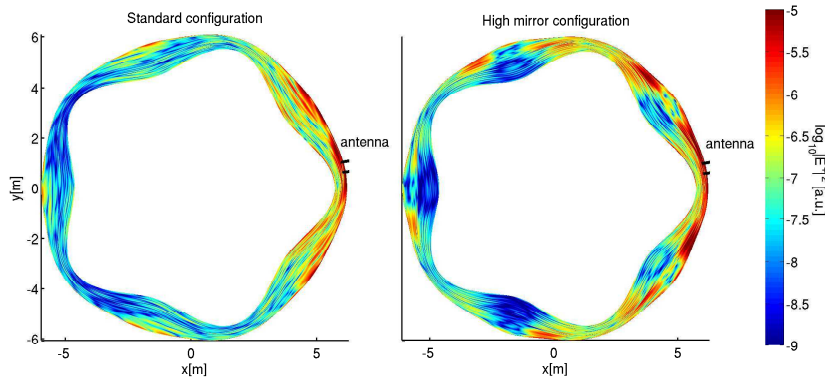


FIGURE 2.  $\log_{10}|E^+|^2$  for each configuration at the torus midplane. The black strokes show the antenna toroidal extension.

The geometrical localisation of the antenna is seen to have a strong impact on the wave propagation in the W7X plasma. In tokamak plasmas the poloidal asymmetry of the equilibrium imposes a strong coupling of the poloidal modes, which is taken into account in the simulations by localising the antenna in the poloidal direction. On the other hand, such plasmas can often be considered axisymmetric resulting in a weak coupling of the toroidal modes. In that case, each toroidal mode of the antenna spectrum can be considered independently from one another. Therefore an approximate model of the antenna surrounds the plasma toroidally for the calculation of each toroidal mode. The wave localisation is found by studying the superposition of a wisely chosen set of modes that sufficiently represent the antenna spectrum. In stellarator plasmas however the equilibrium imposes a strong coupling on both the poloidal and

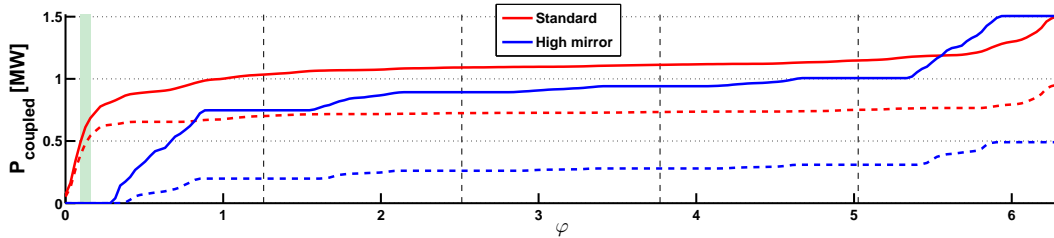
toroidal modes, which is taken into account in the present simulations by localising the antenna in the poloidal and toroidal directions. The wave localisation is seen in Figure 2 via the electric field, which is stronger in amplitude in the period containing the antenna (and in the adjacent period closest to the antenna) than the other periods opposite to the antenna. The observed breaking of five-fold symmetry can be understood by noting that wave energy is transferred at a resonant layer. The wave amplitude is therefore expected to be damped as it travels away from the antenna and encounters resonant layers. Figure 2 also shows that the wave toroidal damping is lower in the high mirror compared to the standard configuration. This can be explained by the strong magnetic field variation in the high mirror configuration which reduces the resonant layers to localized positions in the toroidal direction, leaving some regions with no wave absorption, i.e. the wave amplitude is maintained. A substantial portion of the wave field can travel from the antenna to the next toroidal periods.

## GUIDING CENTRE ORBITS CALCULATION

The guiding centre particle orbit solver VENUS-LEVIS initialises minority species markers following an isotropic Maxwellian distribution function. Those markers are then pushed in time and Monte Carlo operators simulate the ICRF acceleration and the Coulomb collisions with the background species. The ICRH Monte Carlo operator uses the normalised electric field and wave numbers previously computed by LEMan. Each marker crossing the ICRH resonant layer receives kicks in velocity and it is therefore possible to quantify using a PIC method the amount of power coupled to the minority species. The input power is set to 1.5MW according to the value expected from the W7X antenna system [1]. The electric field is regularly adjusted throughout the simulation in order to keep the coupled power constant. The cumulative deposited power over the toroidal angle, integrated over the radial and poloidal directions is computed for both equilibria and displayed in figure 3 :

$$P_{coupled}(\varphi) = \int_0^\varphi \frac{\sum_i w_i \Delta E_i^{ICRH}}{\Delta t} d\varphi' \quad (2)$$

In equation 2,  $i$  labels the markers being between  $\varphi'$  and  $\varphi' + \Delta\varphi'$  during the time interval  $\Delta t$ ,  $w_i$  refers to the markers' numerical weight and  $\Delta E_i^{ICRH}$  is the kick in energy from the ICRH Monte Carlo operator.



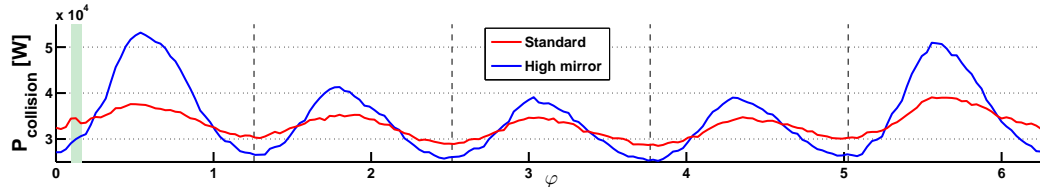
**FIGURE 3.** Cumulative (over toroidal angle) coupled power to the minority species over the whole (full lines) and the inner fourth (dashed lines) of the plasma volume for each configuration. The dashed lines shows each toroidal segment's limits and the green rectangle represents the antenna domain.

Figure 3 confirms that 1.5MW were indeed coupled to the minority species. The periodicity breaking appears also in this diagnostic : most of the power is deposited in the first and last toroidal segments.  $P_{coupled}$  is flat in domains where the resonant layer has vanished. These regions can clearly be observed for the high mirror equilibrium (blue curves). The power deposition is more evenly spread in the standard equilibrium case where no resonance-free region exists (red full curve). Central power deposition is more efficient in the standard equilibrium than in the high mirror equilibrium. About two thirds of the total coupled power is located in the plasma centre (dashed red curve).

The collisional power transferred to the background species (electrons and  $^4\text{He}$  ions) is quantified as :

$$P_{collision}(\varphi) = - \frac{\sum_i w_i \Delta E_i^{Coulomb}}{\Delta t} \quad (3)$$

In equation 3  $\Delta E_i^{Coulomb}$  is the particle energy loss due to the collision with the background species. Figure 4 displays the calculation of  $P_{collision}$  for each configuration. The two curves show peaks in the collisional power in all toroidal segments. They are located in the regions near the triangular cross sections. W7X can be considered as five mirror



**FIGURE 4.** Power transferred to the background species (electrons and  $^4\text{He}$  ions) via Coulomb collisions. The dashed lines shows each toroidal segment's limits and the green rectangle represents the antenna domain.

machines closed in a loop so that low magnetic field regions, i.e. near the triangular cross sections, are accessible to more particles than high magnetic field regions, i.e. near the bean-shaped cross sections. Moreover for the high mirror configuration, the resonant layers are located only in the low field regions explaining the high collisional power in these regions (blue curve in figure 4). A peak in the collisional power appears for the standard configuration in the antenna domain and can be explained by invoking the particle trapping mechanism due to ICRH. The main contribution of ICRH to a resonant particle's velocity occurs in the perpendicular direction relative to the equilibrium magnetic field so that after many wave-particle interactions it typically becomes trapped and its bounce points will be aligned with the resonance position. In the standard configuration a resonant layer exists in the antenna domain, which is also the region where the electric field amplitude is the highest. Many particles interacting with the wave in this region become blocked or localised [10] and their bounce tip aligns in front of the antenna. The heating power density presents a local maximum in this antenna domain explaining the peak in collisional power. Finally figure 4 shows that the high mirror configuration traps the heating power within the segments containing the antenna and in the adjacent one because this magnetic configuration allows less particle transfer between segments than the standard configuration.

## SUMMARY

The 3D full-wave code LEMan was used to compute a realistic ICRF wave field in W7X. The particle orbit solver VENUS-LEVIS was used to compute the interaction between this wave and minority species ions. These simulations show that even if the localisation of the antenna in one segment tends to break the five-fold periodicity of W7X, a low mirror configuration allows the redistribution of the heating power between the segments. Self-consistent simulations will be performed to assess the mutual interaction of the minority species ions distributions and the wave field.

## ACKNOWLEDGMENTS

The calculation presented in this work were undertaken at the CSCS, Lugano, Switzerland under project ID:s493, at IFERC, Rokkasho, Japan. This work was supported by EPFL through the use of the facilities of its Scientific IT and Application Support Center. This work has been carried out within the framework of the EUROfusion Consortium and has received funding from the Euratom research and training programme 2014-2018 under grant agreement No 633053. The views and opinions expressed herein do not necessarily reflect those of the European Commission.

## REFERENCES

1. J. Ongena et al. 2014 *Phys. Plasmas* **21** 061514
2. A. Messiaen et al. 2014 *AIP Conf. Proc.* **1580** 354-357
3. M. Jucker et al. 2011 *Comput. Phys. Comm.* **182** 912-925
4. W. A. Cooper et al. 2009 *Comput. Phys. Commun.* **180** 1524
5. P. Popovich et al. 2006 *Comput. Phys. Commun.* **175** 250
6. N. Mellet et al. 2010 *Comput. Phys. Commun.* **182** 570
7. D. Pfefferle et al. 2014 *Comput. Phys. Commun.* **185** 3127
8. J. Geiger et al. 2008 *35th EPS Conference on Plasma Phys. Hersonissos, 9-13 June 2008* **32D** 2.062
9. J.M. Faustin et al. 2014 *Journal of Physics : Conference Series* **561** 012006
10. A. Gibson et al 1967 *Phys. Fluids(1958-1988)* **10** 2653